2. INSTRUMENTATION AND SAMPLE PREPARATION

commercial Anton Paar flat-plate heating stage connected to an automated RH control system similar to that shown in Fig. 2.9.6. The rapidly collected *in situ* data (30 s per scan, with a position-sensitive detector) were crucial to define at what temperatures longer data collections had to be taken in order to acquire single-phase, high-quality powder patterns suitable for crystal structure solution. Robertson & Bish (2010) managed to index and solve the dihydrate and tetrahydrate phases by charge flipping. Although the tetrahydrate structure was later revised by Solovyov (2012) using the exact same data, this example clearly indicates the level of complexity that can be studied in local laboratories under *in situ* conditions. In this case, this task included understanding the dehydration pathway, solving the structure of $Cl_2H_4MgO_{10}$ with two molecules in the unit cell and refining anisotropic displacement parameters using Rietveld refinement.

2.9.3.3.3. *Large-volume cells for energy-dispersive diffraction*

Large-volume cells have been used to date with great success almost exclusively with energy-dispersive diffraction (EDXRD). Early work on this was carried out by Munn *et al.* (1992) and He *et al.* (1992) using the synchrotron source at Daresbury Laboratory. Walton & O'Hare (2000), who continued the pioneering work, provide a good historical overview of the kinds of studies that can be performed. Norby (2006) also provides excellent references to and explanations of work in this field. In brief, the main advantages of EDXRD are that the X-ray high energies (*i.e.* 50–120 keV) present in the beam can penetrate and probe into large vessels. Furthermore, only minor modifications to create small entrance and exit windows on commercial autoclaves, which are standard equipment in many laboratories, are necessary in order to turn them into extreme-condition *in situ* reaction vessels. An additional advantage arises from the fact that there is no bias due to volume differences between the laboratory experiments and *in situ* reactions studied at the synchrotron (see Fig. 2.9.8).

The variety of scientific applications is huge: pressure-induced phase transitions of inorganic solids, hydrothermal synthesis of microporous solids, intercalation, growth of layered perovskites and breathing in metal-organic frameworks, to name a few examples (see Walton & O'Hare, 2000). Extreme conditions can be reached in terms of temperature ($\sim$1273 K) in an autoclave with subsecond XRD time resolution. EDXRD in combination with large-volume autoclaves has provided otherwise-inaccessible information on many processes: intermediates in crystallization routes, activation energies for reactions, and kinetic parameters crucial for their understanding and optimization. The major disadvantage of EDXRD is that the resolution in the diffraction pattern is limited, since it is defined by the energy resolution of the solid-state detector. This effectively excludes all access to precise structural information. However, recent efforts have allowed quantitative phase analysis (Rowles, 2011; Rowles *et al.*, 2012). With the advent of third-generation synchrotrons, which provide orders of magnitude more flux at high energies, and the availability of high-energy flat-panel detectors, angular-dispersive diffraction data can successfully be collected from samples in large-volume cells. Their use expands the available information dramatically. To date, however, there are very few high-energy angular-dispersive beamlines, and the use of the large-volume cells in combination with EDXRD remains an active field and has recently been developed further by, for example, Moorhouse *et al.* (2012) at the Diamond Light Source. The cell there can be equipped with various reaction vessels made of alumina, steel, PTFE-lined steel or glassy carbon tubes depending on the chemical reaction to be studied. It can achieve temperatures as high as 1473 K with infrared lamps and has a magnetic stirrer to avoid sedimentation of the reaction products. In addition, Styles *et al.* (2012) have developed a large furnace and *in situ* cell for salt electrolysis.

Rijssenbeek *et al.* (2011) have studied a full-size battery cell with EDXRD (see Fig. 2.9.9). Diffraction data were collected during charge/discharge at high temperature of the sodium metal halide (Na/MCl$_2$, M = Ni and/or Fe) cells. They were able to assess the charge-state variations as a function of space and time in the cell during many charge/discharge cycles, and identify local crystal structures and phase distributions. The data confirm the propagation of a known well-defined chemical reaction front beginning at the ceramic separator and proceeding inward.

2.9.3.3.4. *Large-volume cells for angular-dispersive diffraction*

This application implies the use of monochromatic X-rays with extremely high energies (70 keV and above). Such energies can be easily reached on third-generation synchrotrons with in-vacuum undulators, thus providing sufficient flux for angular-dispersive diffraction experiments. The challenge with these experiments is to have a sufficiently high X-ray energy to penetrate large sample-cell vessels while maintaining reasonably good angular resolution in the diffraction pattern. When using large *in situ* cells with low-energy diffraction, there is a severe peak-broadening effect resulting in a deterioration of the data quality. At high energies, however, where the scattering angles are small, the sample thickness has little effect on the angular resolution provided that the area detector is positioned at a sufficient distance from the sample.
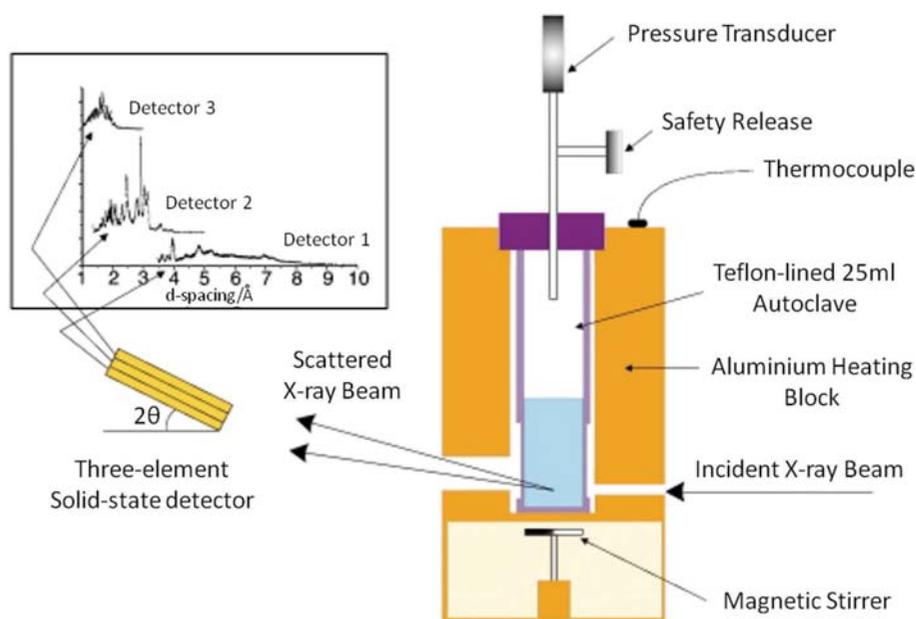

Figure 2.9.8
A schematic of the Oxford/Daresbury hydrothermal autoclave used for energy-dispersive X-ray diffraction studies. Adapted from Walton & O'Hare (2000) with permission of The Royal Society of Chemistry.

O'Brien *et al.* (2011) explain the trade-offs for such experiments in detail and have shown that it is possible to extract useful structural information. Large-volume cells that used to be exclusively the domain of neutron diffraction and EDXRD have now also been adapted for angular-dispersive powder diffraction with, in some cases, increased speed and information content. For instance, Wragg *et al.* (2012) studed an industrial methanol-to-olefin conversion process with *operando* time- and space-resolved diffraction. The sample is rapidly scanned up and down to provide one-dimensional spatial information. The results complement earlier experiments performed with a microreactor. Jacques *et al.* (2011) extracted three-dimensional information by using dynamic X-ray diffraction computed tomography (XRD-CT). They measured over 50 000 diffraction patterns on beamline ID15 at the ESRF with different sample orientations, positions and temperatures. From this huge amount of data, they reconstructed the catalyst body in three dimensions with a diffraction pattern assigned to each volume unit within the sample as a function of time. With this information, they were able to follow the evolution of the catalytically active phase throughout the sample. Wragg *et al.* (2015) have since performed Rietveld analysis on voxels from the XRD-CT data for a methanol-to-olefin reactor bed. It is also worth mentioning work by Jensen *et al.* (2007), performed on beamline 1-ID at APS Argonne National Laboratory, investigating the kinetics of nanoparticle formation involving a sol–gel reaction in supercritical CO_2 at 10 MPa. The reaction was studied with XRD and small-angle X-ray scattering (SAXS) in a large 30 ml vessel. In a different application, Friščić *et al.* (2013) mounted a laboratory-scale 10 ml ball mill on the ID15 beamline in order to study mechanochemical reactions, which are used in numerous industrial production processes. By averaging ten 400 ms frames, they obtained sufficiently good data to perform full-pattern refinements and kinetic analysis, providing information about otherwise completely inaccessible processes. We therefore foresee a bright future for such extreme high-energy applications together

with large-volume studies, since they provide a useful bridge between the academic and industrial worlds.

2.9.3.4. *Cells specifically for neutrons*

2.9.3.4.1. *Introduction*

The special characteristics of neutrons imply both advantages and challenges for the design of *in situ* experiments and their associated equipment. The differences in penetration depths between X-rays and neutrons and the correspondingly smaller scattering cross sections for neutrons, together with the much lower flux densities, imply that cells for neutrons are quite different from the miniature capillary cells for X-rays described in the previous sections. Above all, the sample volume is by necessity often much larger than the equivalent volume required for a laboratory X-ray or synchrotron experiment. However, the ability of neutrons to penetrate deep into sample environments has been of great importance for studying samples at very low temperature, under high pressure or within strong magnetic fields. Similarly, reaction cells for *in situ* investigations profit from the ability of neutrons to penetrate through thick-walled vessels, for example for studying gas–solid reactions under high pressure. Only relatively recently, with the availability of high-energy synchrotron beamlines (>100 keV), can X-rays effectively compete with neutrons in this domain. Even in these cases, the very different scattering properties of neutrons (*e.g.* the strong variation of cross section with isotope) means that some measurements that are challenging, if not impossible, with X-rays can become quite feasible with neutrons. The solid–gas reaction of intermetallic phases with H_2 gas is a good example, where the positions of the interstitial H atoms can be located within a heavy-metal hydride (Kamazawa *et al.*, 2013). Similarly, the hydration of cement has been investigated many times, with improved time resolution resulting from developments in neutron optics and detector performance. *In situ* studies of oxidation reactions have also benefited from the better ability of
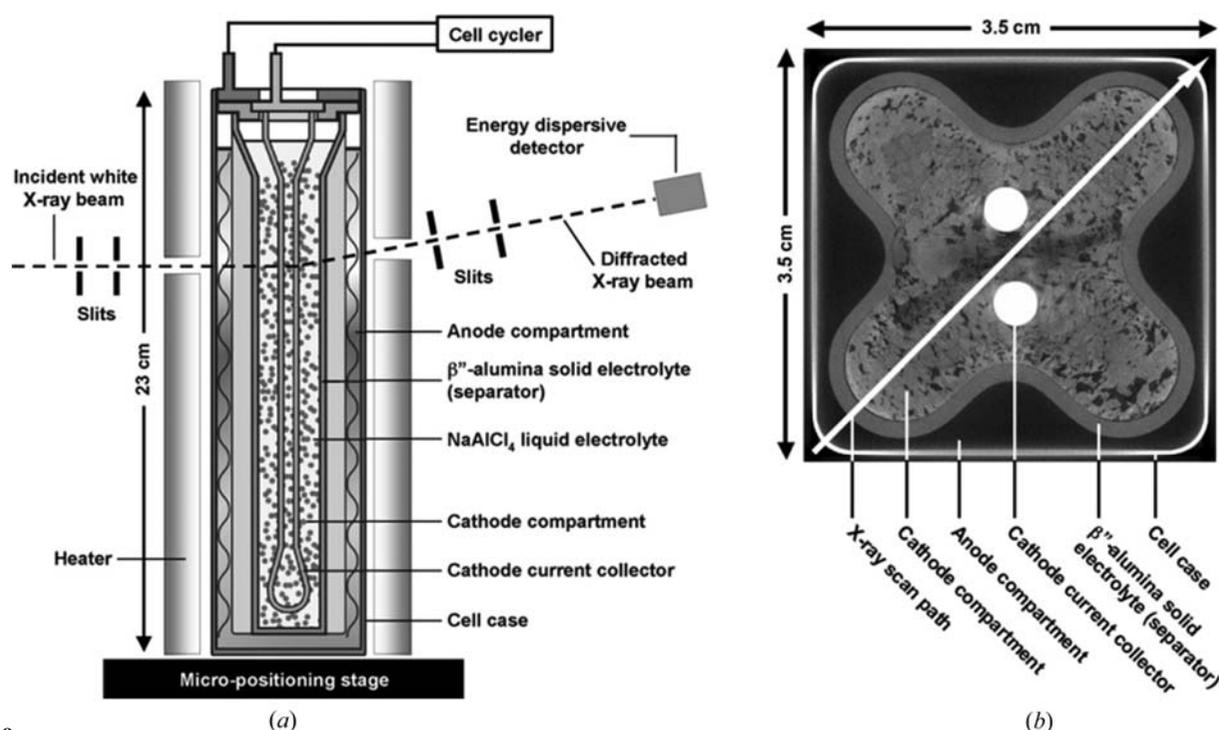

(*a*) (*b*)

Figure 2.9.9
(*a*) Schematic of a sodium-halide cell in an *in situ* synchrotron EDXRD experimental setup. (*b*) Cross-sectional computed tomography image of a cell. The arrow along the cell diagonal denotes the path of the X-ray line scans used in this work. This corresponds to an X-ray penetration depth of up to 50 mm. Adapted from Rijssenbeek *et al.* (2011) with permission from Elsevier.